Electronic Supporting Information

Enhanced stability and complex phase behaviour of organic-inorganic green-emitting ionic manganese halides

*Brando Adranno, Veronica Paterlini, Volodymyr Smetana, Guillaume Bousrez, Alexander Ovchinnikov and Anja-Verena Mudring**

Content:

I. Infrared spectra (IR)

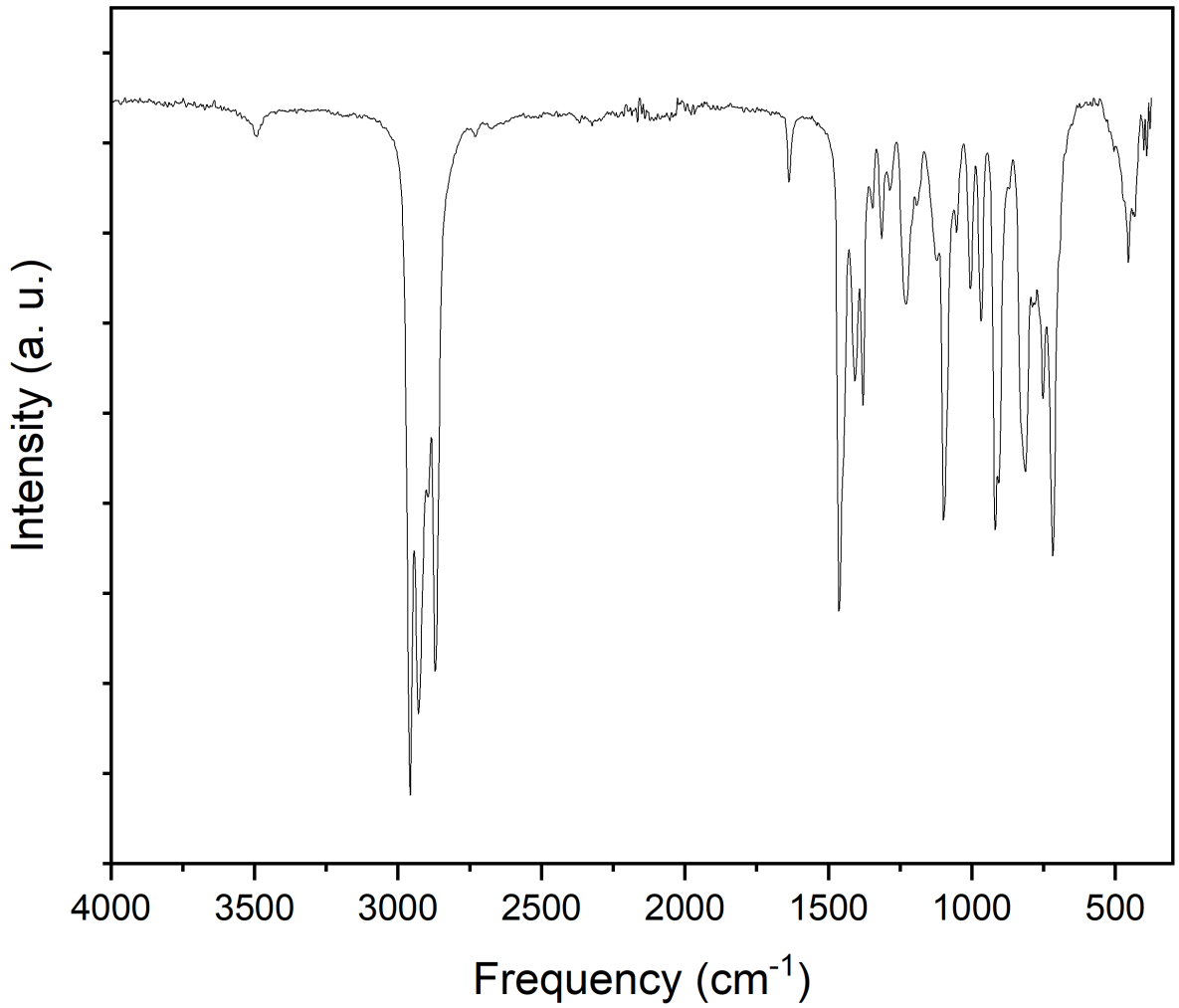

Figure S1. IR spectrum of **1**.

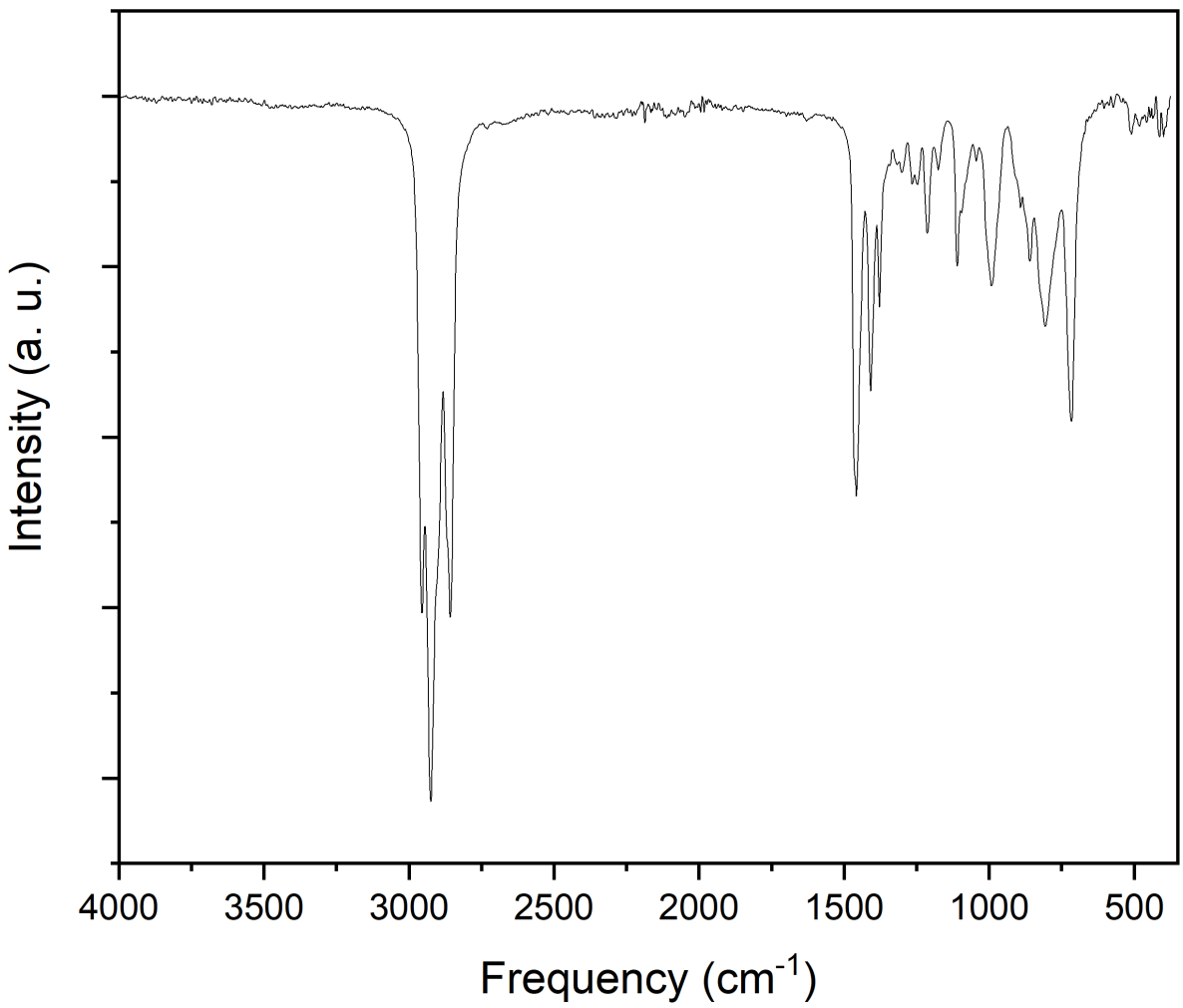

Figure S2. IR spectrum of **2**

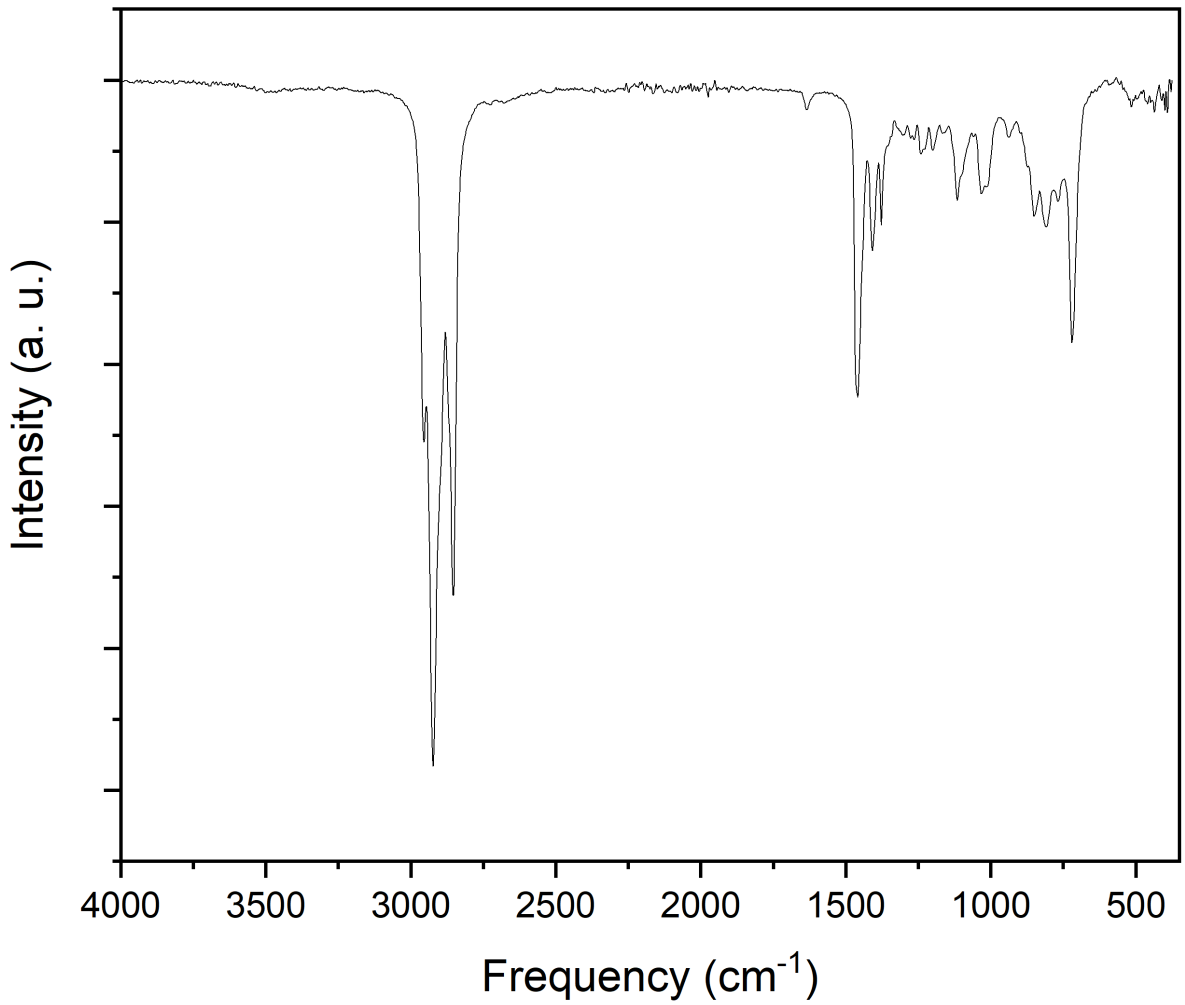

Figure S3. IR spectrum of **3**

II. Karl-Fischer titration results

Table S1. Water content of **1**-**3** when exposed to ambient atmosphere for several months as determined by Coulometric Karl-Fischer titration.

Compound	Water content (mol%)
1	0.35
2	0.12
3	0.25

III. Raman spectra

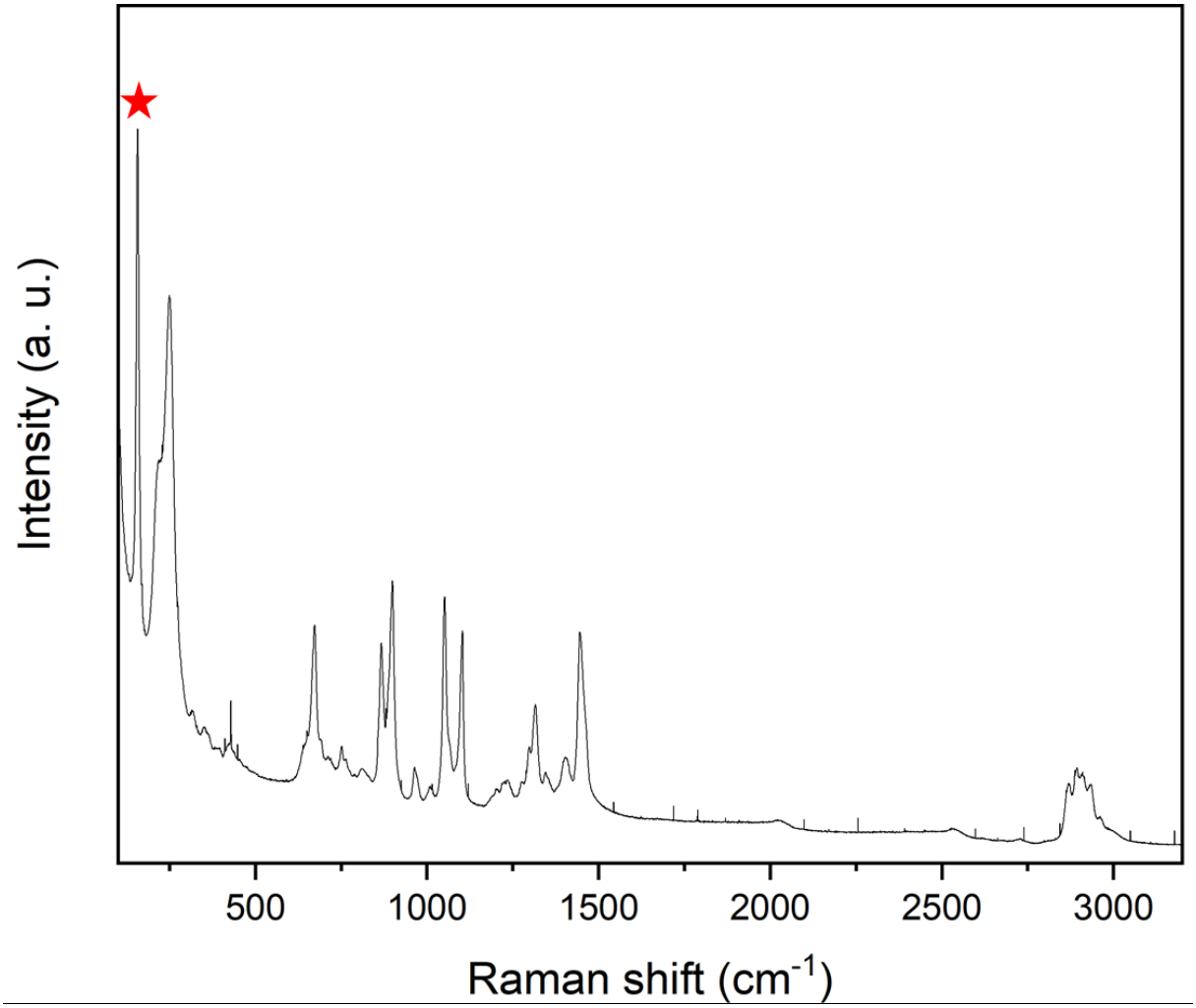

Figure S4. Raman spectrum of **1**. The totally symmetric A_1 Mn-Br stretching mode is marked with a *red* star.

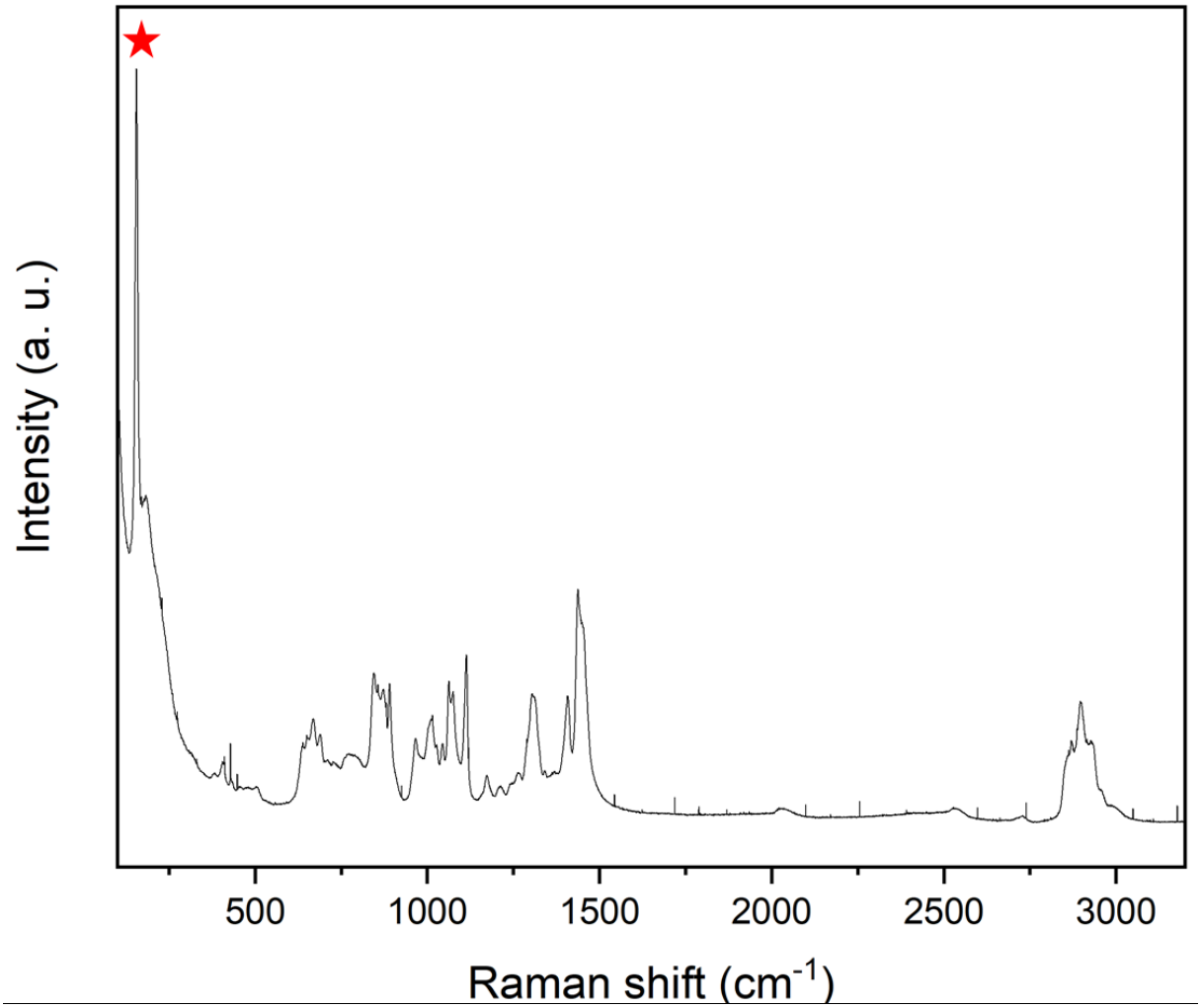

Figure S5. Raman spectrum of **2**. The totally symmetric A_1 Mn-Br stretching mode is marked with a *red* star.

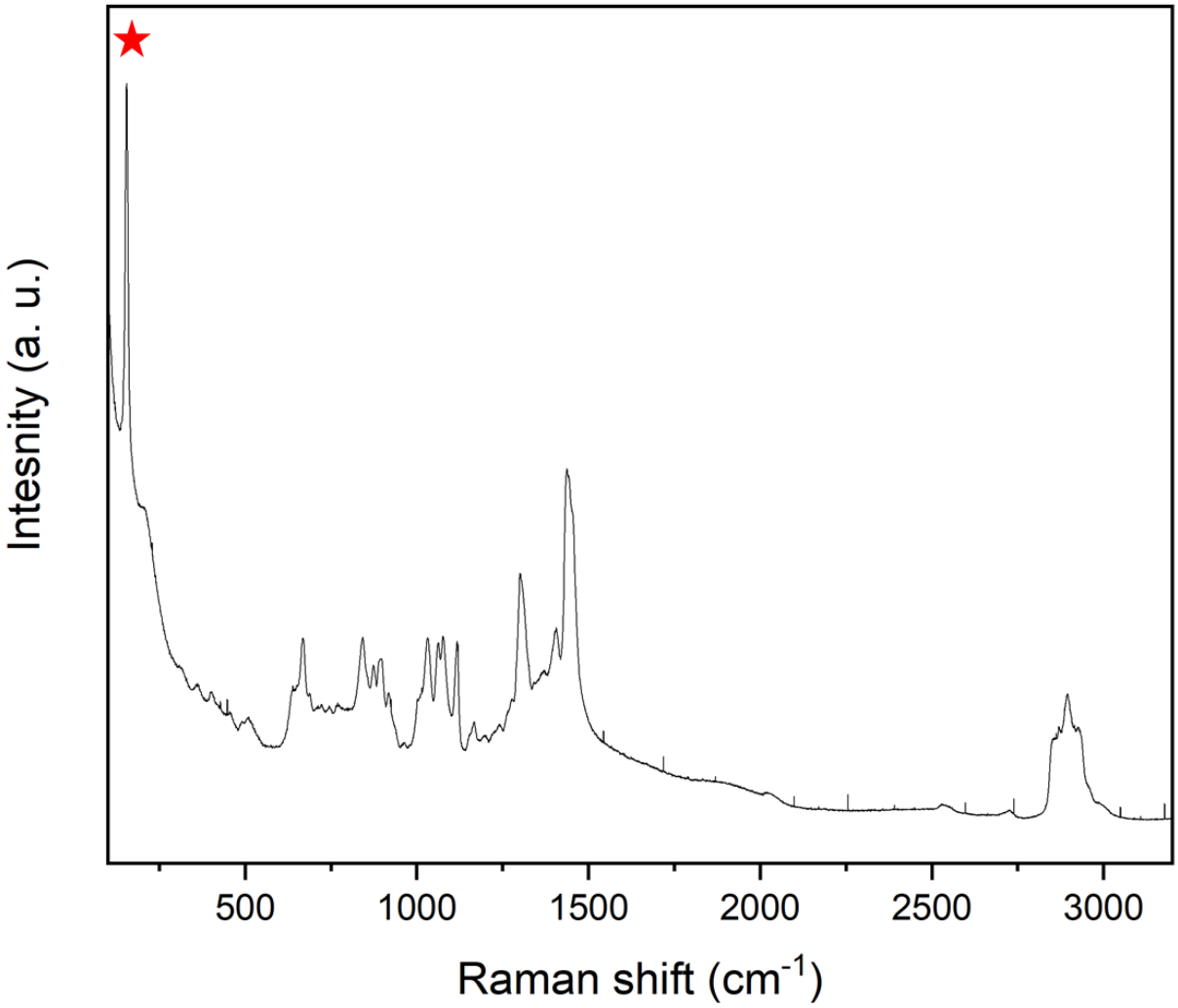

Figure S6. Raman spectrum of **3**. The totally symmetric A_1 Mn-Br stretching mode is marked with a *red* star.

IV. Crystallographic details

Table S2. Crystallographic data of **1**.

Compound	**$[P_{4444}]_2[MnBr_4]$**
CCDC	2115615
Formula	$C_{32}H_{72}Br_4MnP_2$
Formula weight [g·mol^{-1}]	893.41
***T* [K]**	100(2)
Crystal system	Monoclinic
SG	$P2_1/c$
***a* [Å]**	17.1007(19)
***b* [Å]**	16.2849(18)
***c* [Å]**	17.357(2)
***β* [°]**	118.394(3)
***V* [Å^3]**	4252.2(8)
Z	4
Density (g/cm^3)	1.396
μ (mm^{-1})	4.163
***F*(000)**	1836
Index ranges	$-21 \leq h \leq 21$ $-20 \leq k \leq 20$ $-21 \leq l \leq 21$
Measured reflections	9979
Unique reflections	8654
Observed reflections	4988
Number of parameters	360
R_{int}	0.1576
***R*, *wR* (all, observed)**	0.0544, 0.1180
$\Delta\rho_{max}$ = (e·Å^{-3})	1.891
$\Delta\rho_{min}$ = (e·Å^{-3})	-1.346

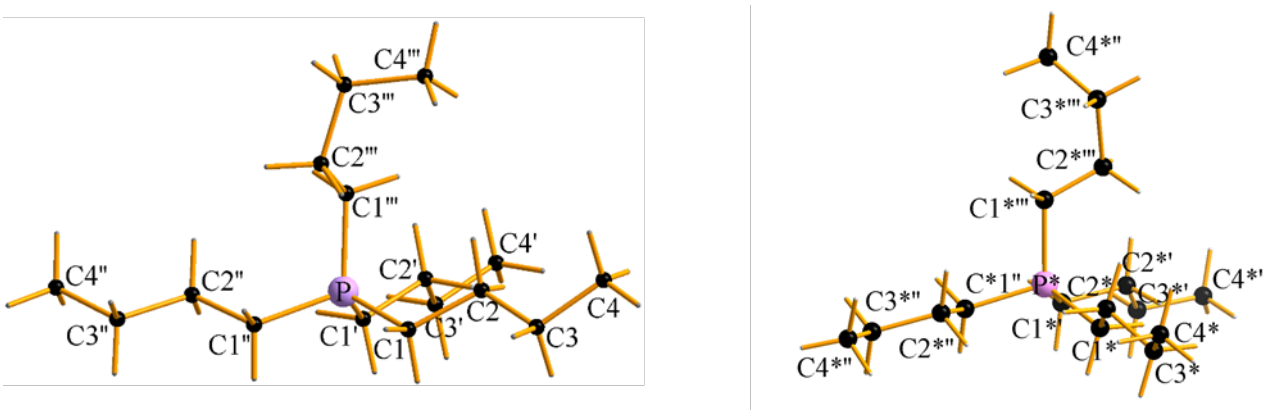

Figure S7. Molecular structure of the two different $[P_{4444}]^+$ cations in the crystal packing of **1**. C atoms are in *black*, P atoms in *purple*, and H atoms in *white* (small spheres).

Table S3. Torsion angles in the molecules of the cations in **1**.

	Torsion angle [°]			
Cation 1, *	C	C'	C''	C'''
PC1*C2*C3*	-175.7(5)	-177.8(5)	-174.7(5)	163.3(5)
C1*C2*C3*C4*	-171.7(6)	178.7(6)	178.7(6)	-77.1(7)
Cation 2, *	C	C'	C''	C'''
PC1*C2*C3*	177.4(5)	179.1(5)	173.8(5)	-167.5(5)
C1*C2*C3*C4*	177.5(6)	-178.1(6)	-176.8(7)	-66.2(9)

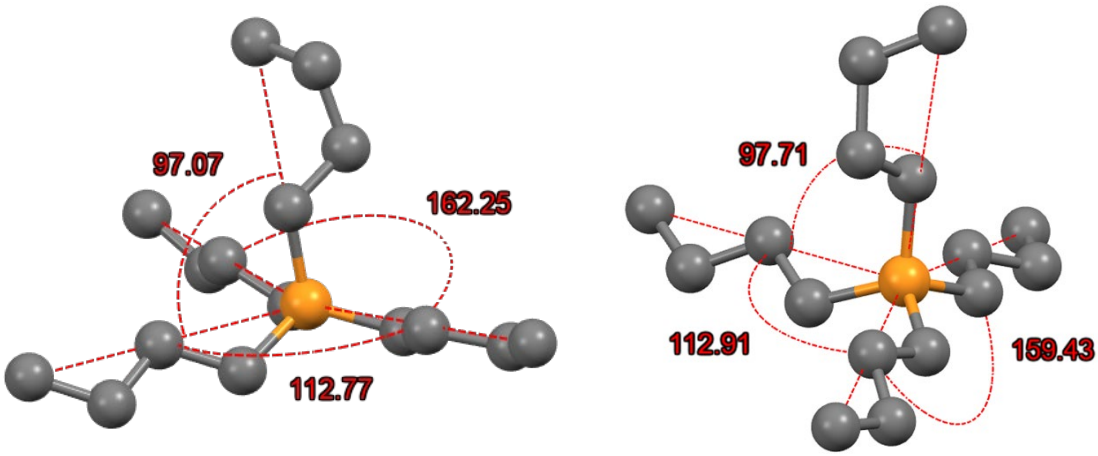

Figure S8. Conformation of the $[P_{4444}]^+$ cations with the angles ∠CH3-P-CH3 (°). P atoms are plotted in *orange*, while C atoms are in *grey* and H atoms are omitted for clarity.

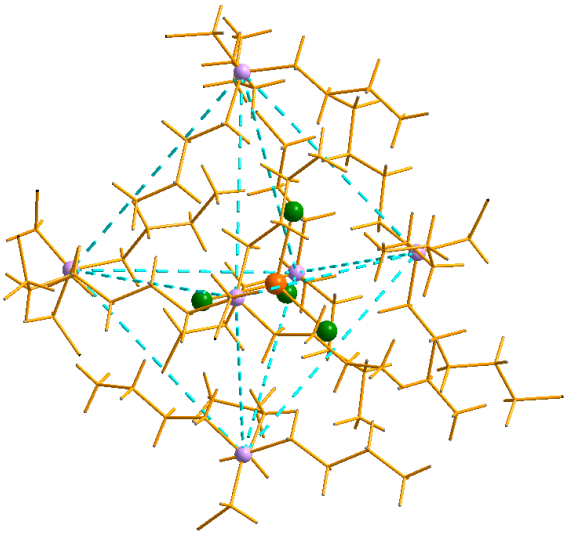

Figure S9. Phosphonium cations of **1** surrounding one $[MnBr_4]^{2-}$ complex in a distorted octahedral arrangement. The sides of the octahedron are in *light blue dashed lines*, the Mn atom is in *orange*, P atoms are in *purple*, Br atoms are in *green*.

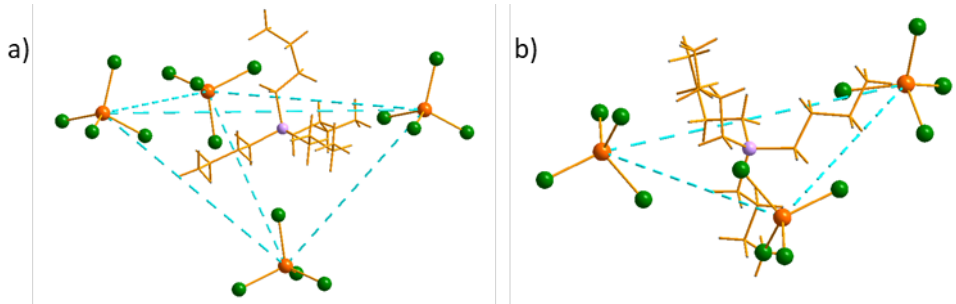

Figure S10. The short contact arrangements of four (*a*) and three (*b*) $[MnBr_4]^{2-}$ surrounding the phosphonium cations. The involved $[MnBr_4]^{2-}$ are connected by *light blue dashed lines*, the Mn atoms are in *orange*, P atoms are in *purple*, Br atoms are in *green*.

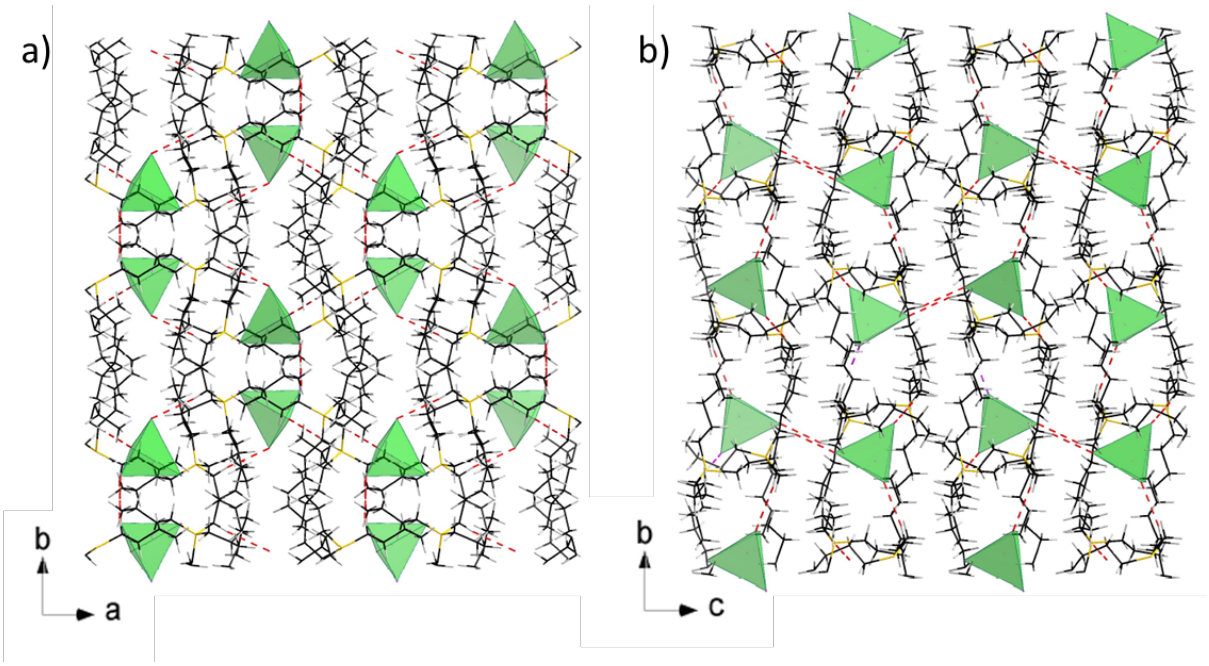

Figure S11. Projection of the crystal lattice of $[P_{4444}]_2[MnBr_4]$ (**1**) in the crystallographic *ab* plane showing the organic wave-like layers (a), and distribution of the isolated $[MnBr_4]^{2-}$ complexes along the crystallographic *a*-axis (b). The C-H---Br bonds are in *red dashed lines*.

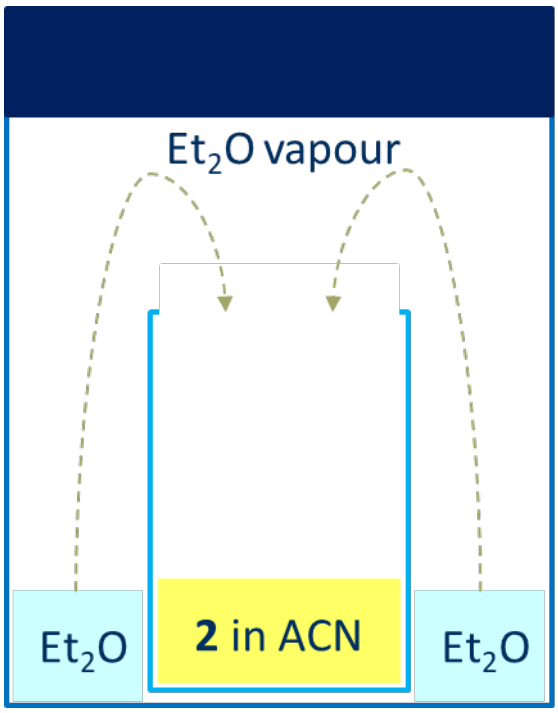

Figure S12. Slow vapor diffusion set up for growth of crystals of **2**.

V. Thermogravimetric analyses (TGA)

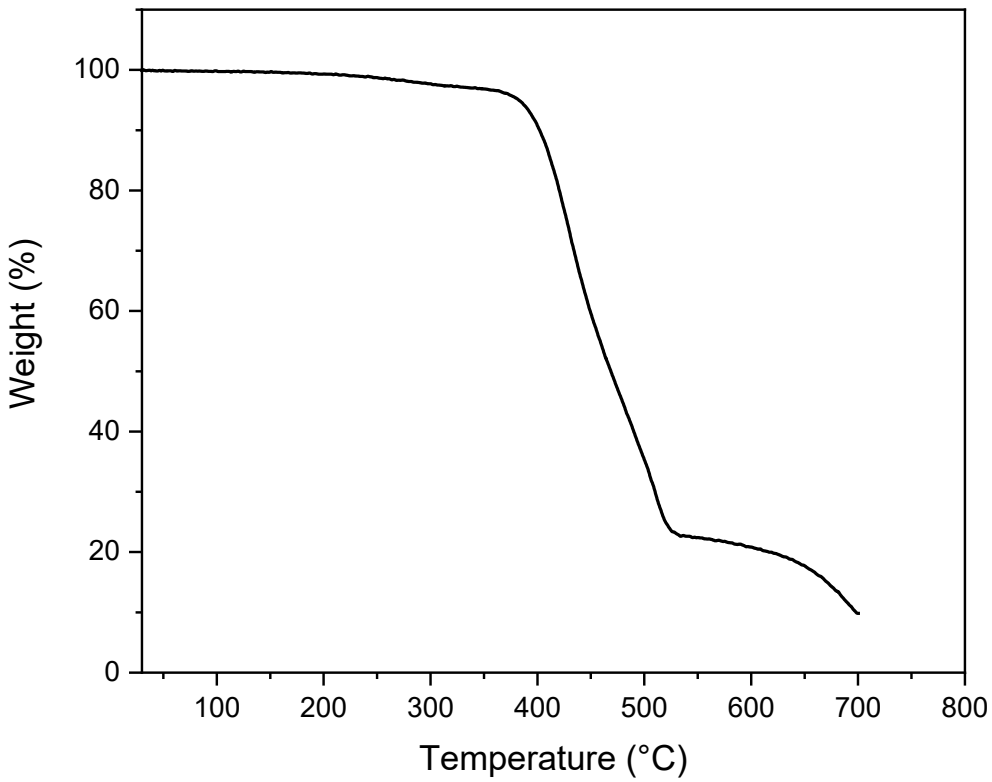

Figure S13. Thermogravimetric profile for **1.**

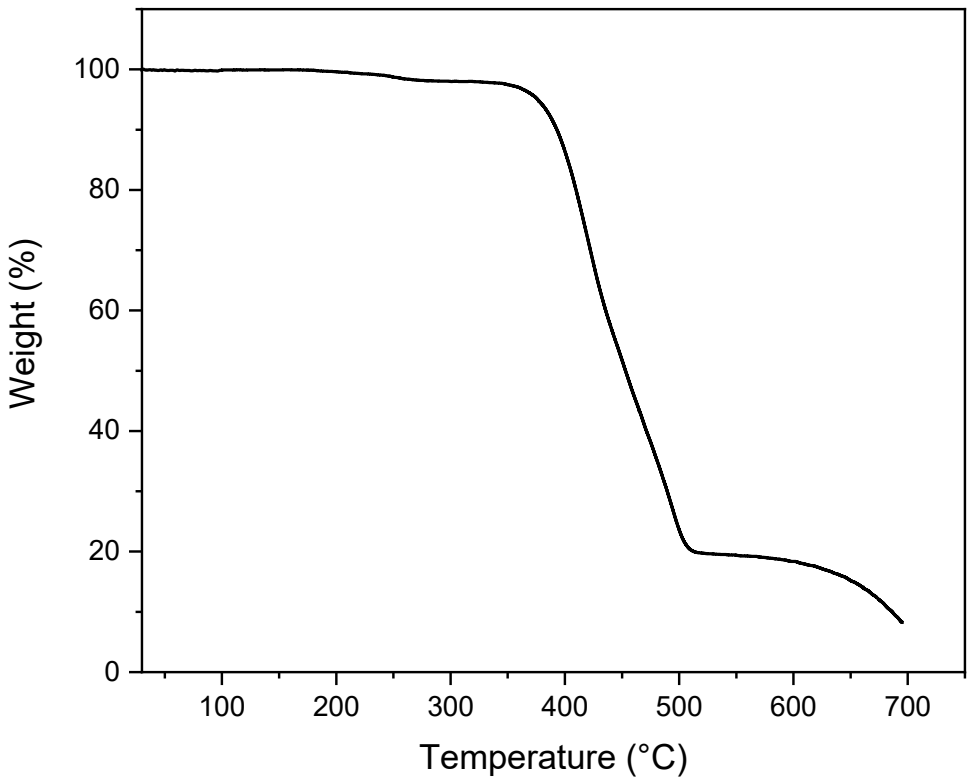

Figure S14. Thermogravimetric profile for **2.**

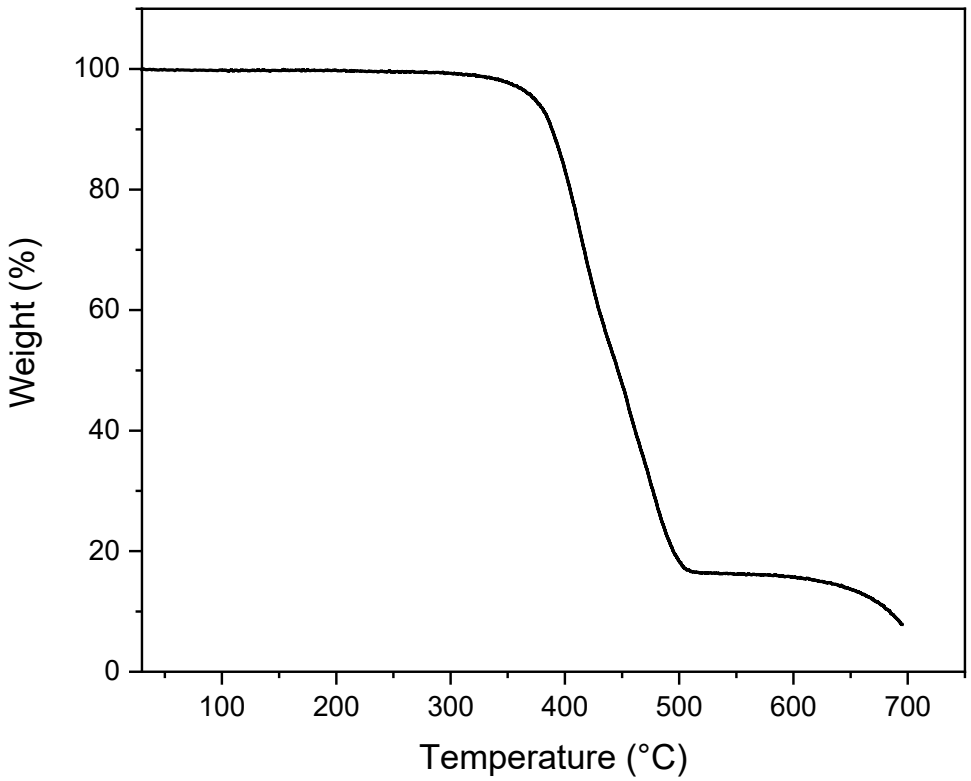

Figure S15. Thermogravimetric profile for **3.**

VI. Differential scanning calorimetry (DSC)

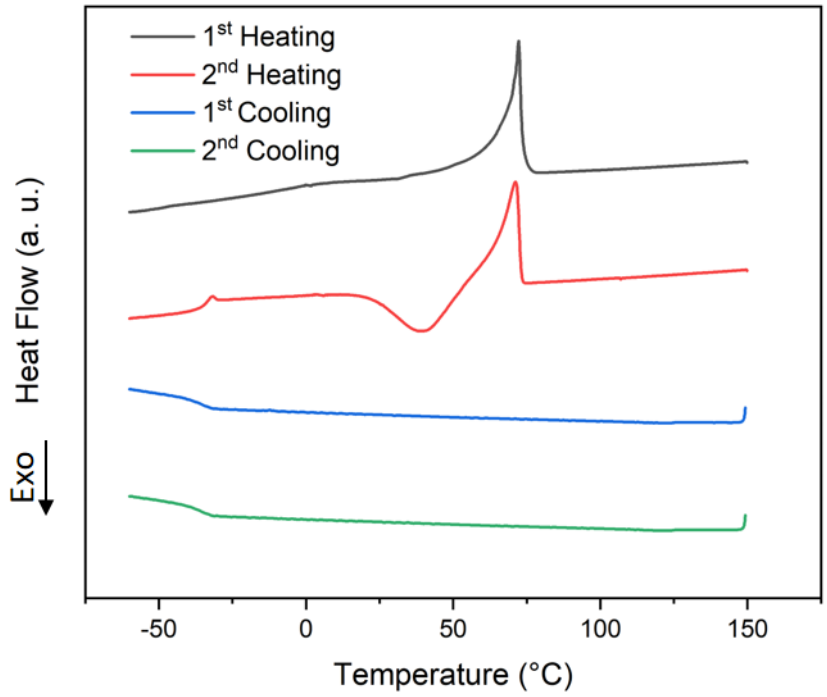

Figure S16. Differential scanning calorimetry curves of **1**.

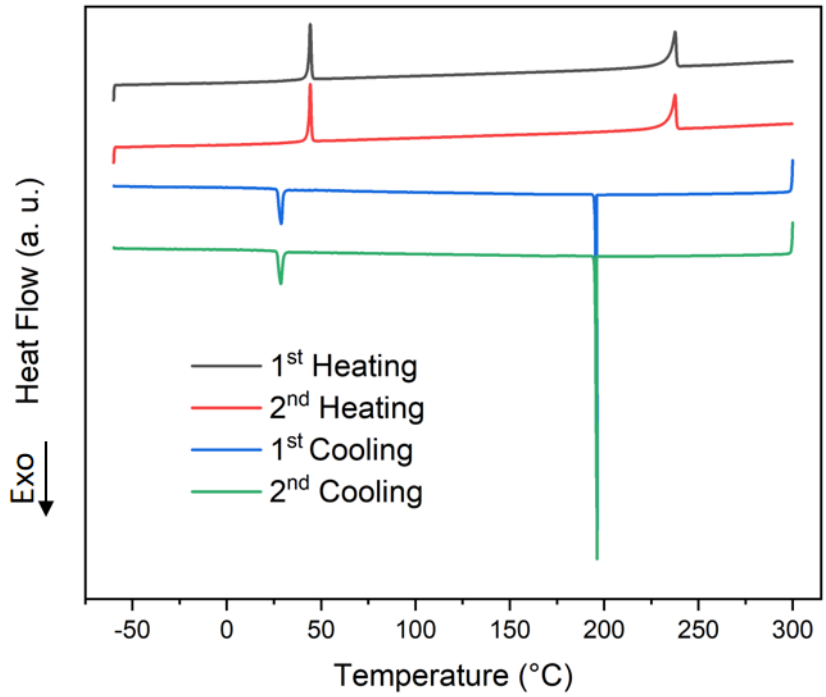

Figure S17. Differential scanning calorimetry curves of **2**.

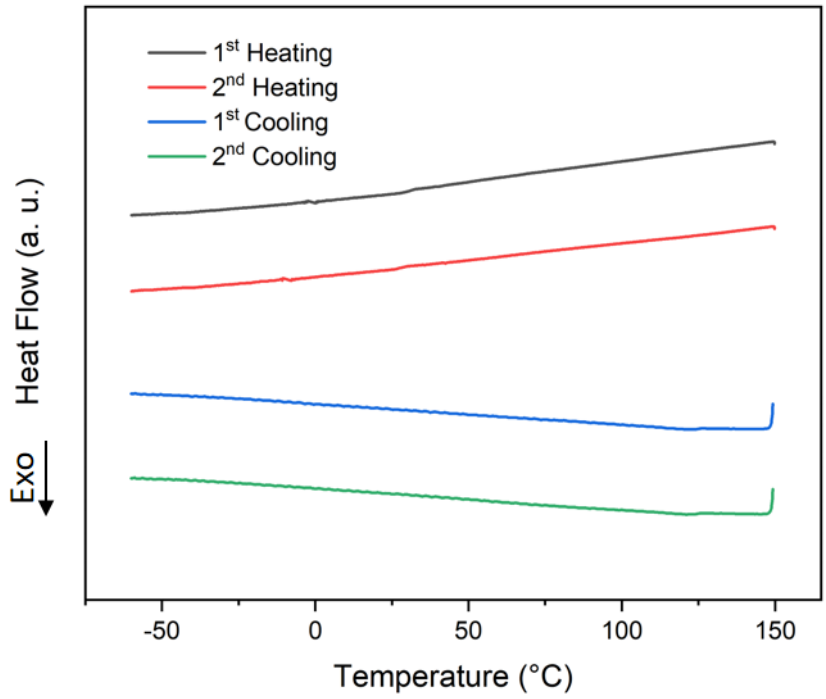

Figure S18. Differential scanning calorimetry curves of **3**.

Table S4. Unit cell parameters of LTS and HTS phases of **2** obtained from indexing of the peaks revealed by PXRD.

Phase	**LTS**	**HTS**
Crystal system	Monoclinic-C	Cubic-F
***a* [Å]**	17.1007(19)	23.628(3)
***b* [Å]**	16.2849(18)	
***c* [Å]**	17.357(2)	
***β* [°]**	118.394(3)	
FOM[a)]	109.0	134.0

[a)] Figure of merit: F_{11} and F_{30} for the cubic and monoclinic forms, respectively, with F_N defined according to Smith and Snyder.[1]

VII. Powder X-ray diffraction (PXRD) data

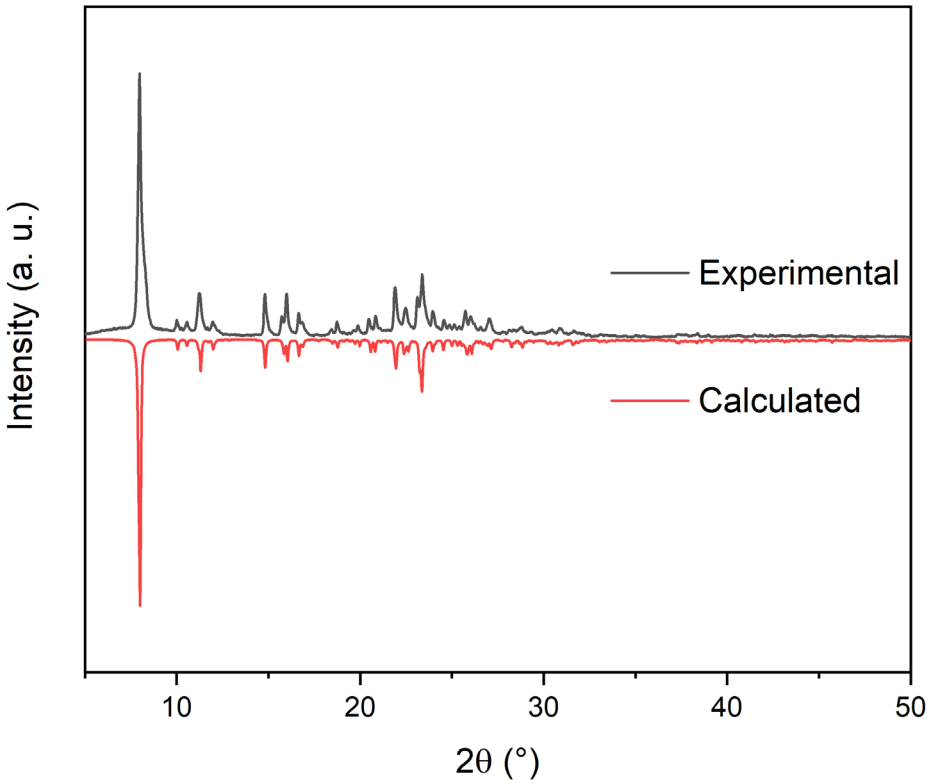

Figure S19. Recorded PXRD from recrystallized **1** together with the pattern calculated from the model refined from the room-temperature single-crystal X-ray diffraction data.

VIII. Absorption spectra

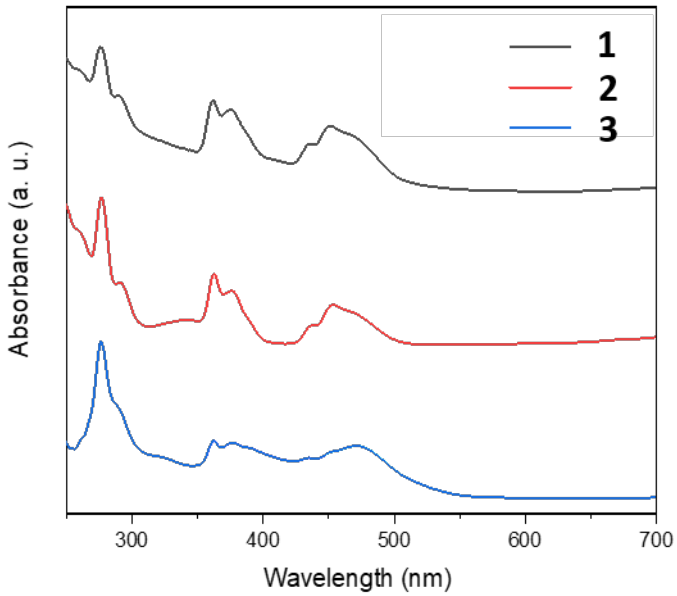

Figure S20. Absorption spectra of **1**-**3**.

IX. Luminescence spectroscopy

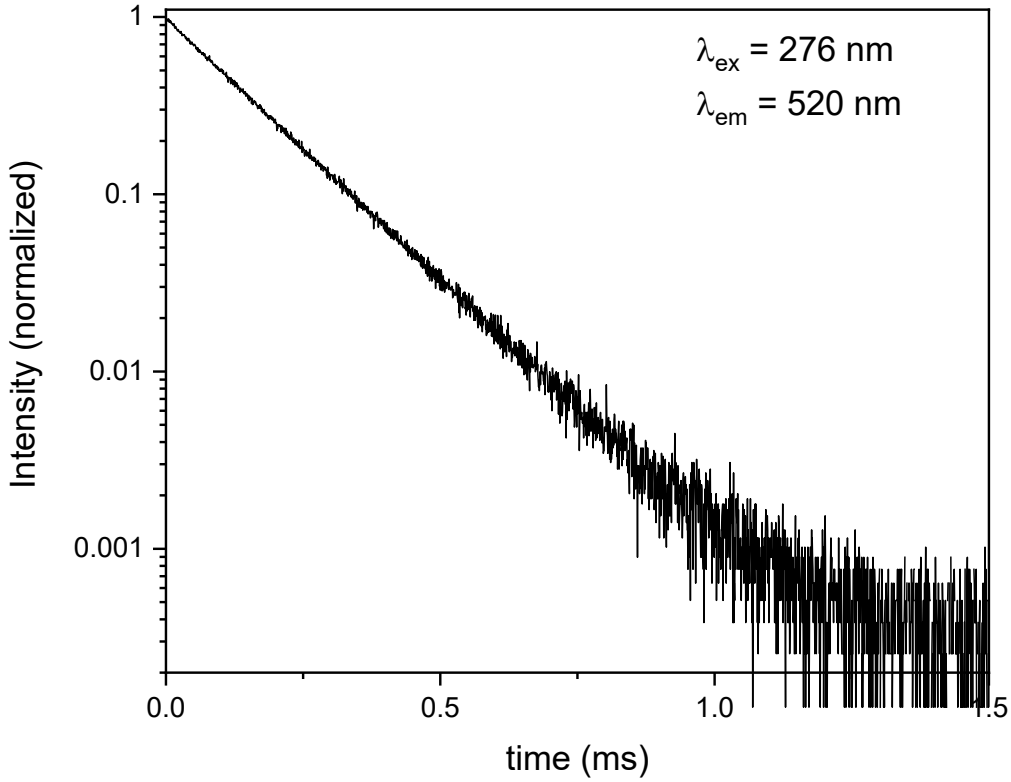

Figure S21. Phosphorescent decay curve for **1** (λ_{ex} = 276 nm).

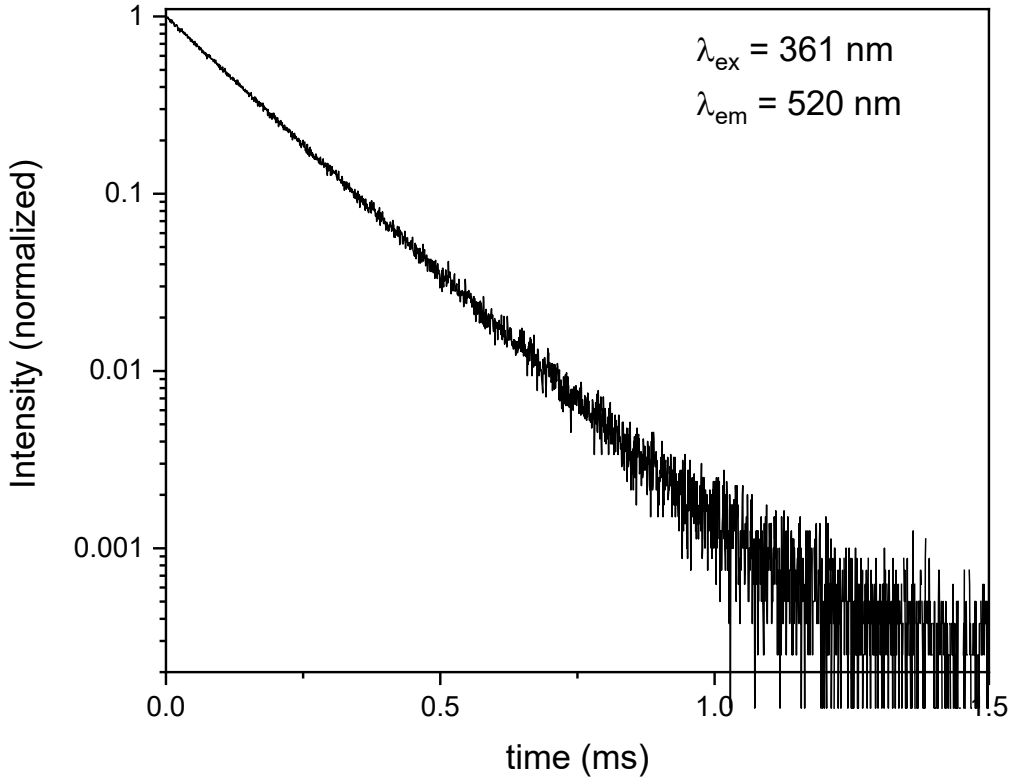

Figure S22. Phosphorescent decay curve for **1** (λ_{ex} = 361 nm).

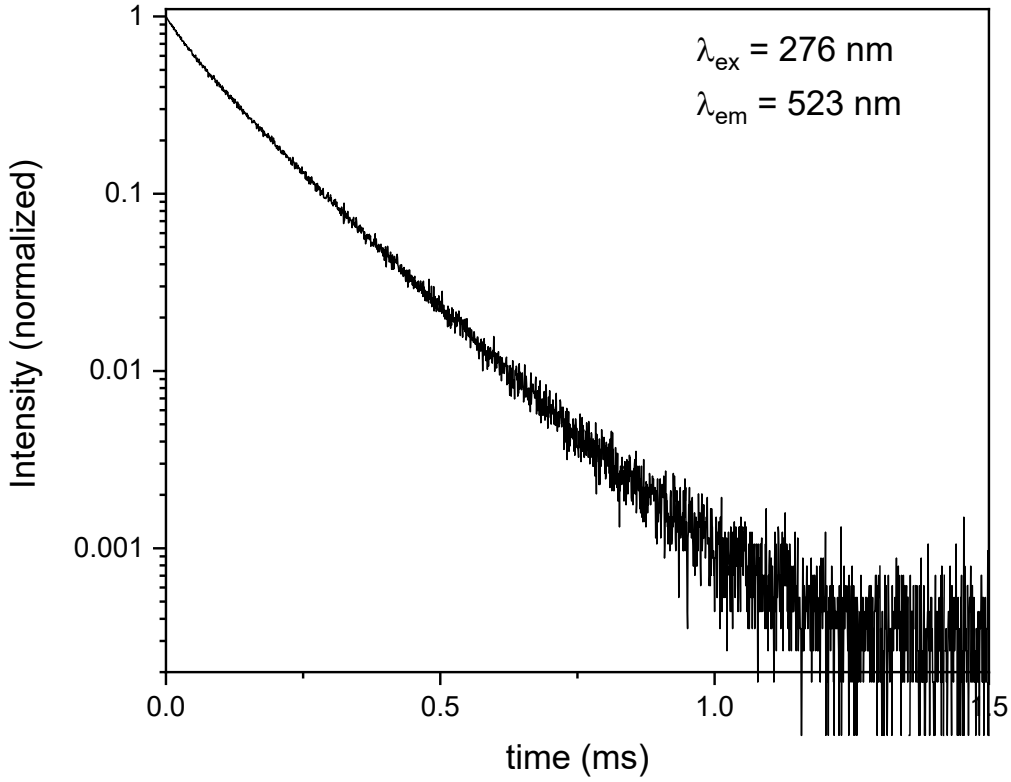

Figure S23. Phosphorescent decay curve for **2** (λ_{ex} = 276 nm).

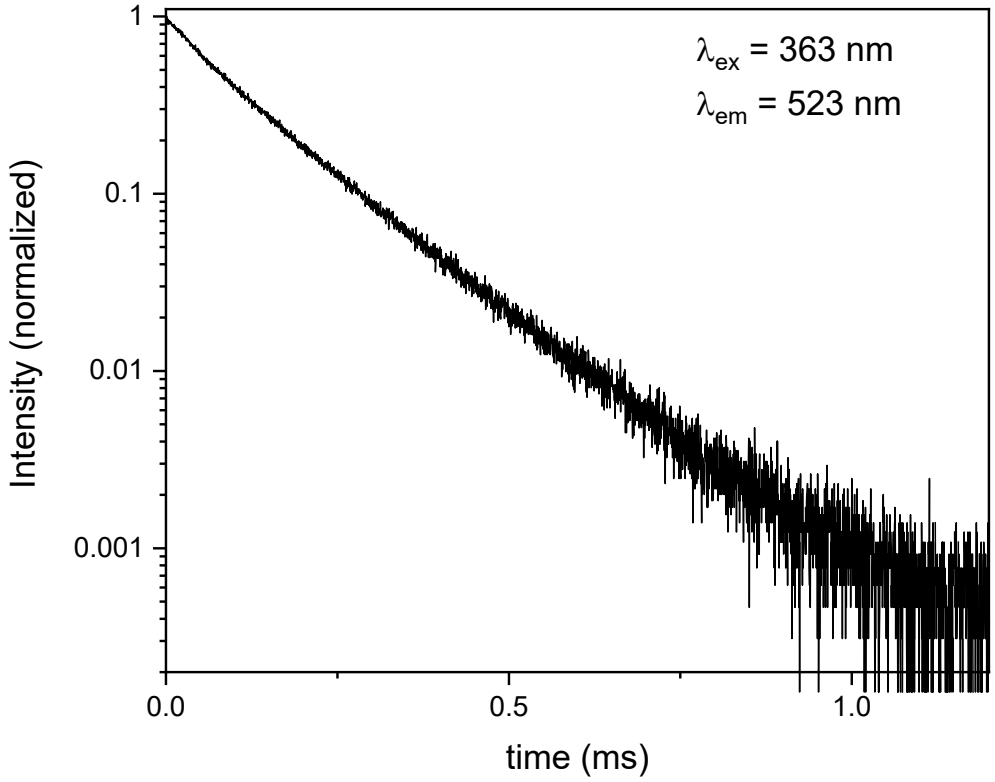

Figure S24. Phosphorescent decay curve for **2** (λ_{ex} = 363 nm).

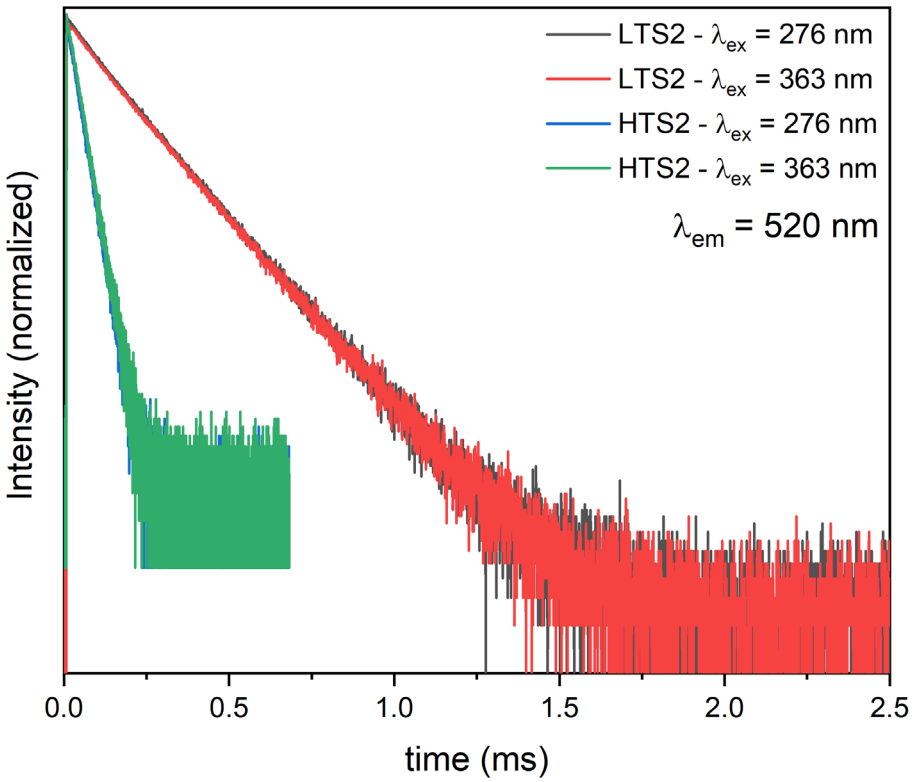

Figure S25. Phosphorescent decay curves for LTS and HTS of **2** during the first heating and cooling cycle. LTS data collected at RT, HTS data collected at 80 °C.

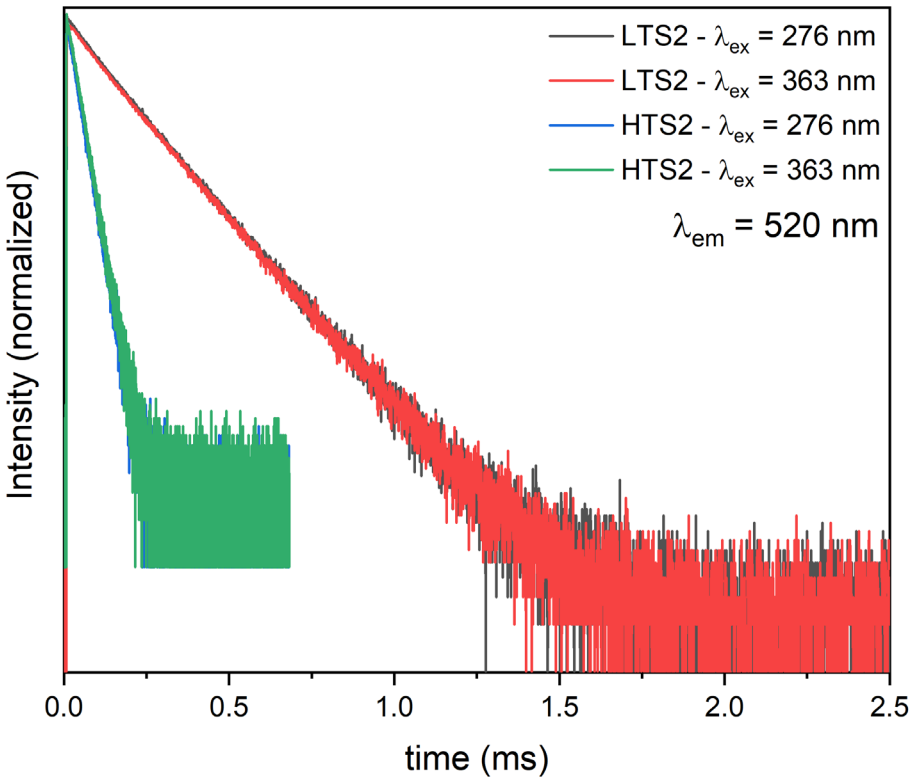

Figure S26. Phosphorescent decay curves for LTS and HTS of **2** during the second heating and cooling cycle. LTS data collected at RT, HTS data collected at 80 °C.

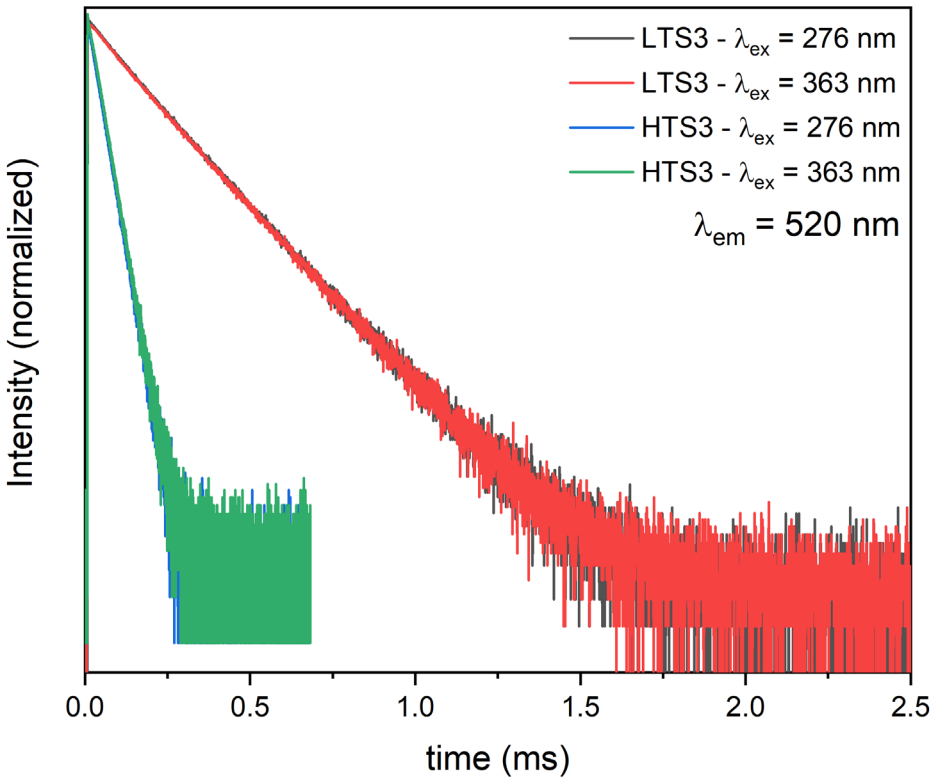

Figure S27. Phosphorescent decay curves for LTS and HTS of **2** during the third heating and cooling cycle. LTS data collected at RT, HTS data collected at 80 °C.

References

1. G. S. Smith and R. L. Snyder, *J. Appl. Crystallogr.*, 1979, **12**, 60-65.